Hindawi
Journal of Applied Mathematics
Volume 2022, Article ID 5732050, 9 pages
https://doi.org/10.1155/2022/5732050

Research Article

Evaluation of Compaction Uniformity of Asphalt Pavement Based on Construction Depth Variation

Xiaodong Jia

School of Urban Construction Engineering, Chongqing Technology and Business Institute, Chongqing 400085, China

Correspondence should be addressed to Xiaodong Jia; huayan063739963@163.com

Received 17 August 2022; Revised 5 December 2022; Accepted 7 December 2022; Published 21 December 2022

Academic Editor: Dan Huang

The continuous monitoring and real-time feedback on the uniformity of the mixture after paving and compaction is important to guide the construction and improve the life of the asphalt pavement. Thus, in this study, the latest digital image technology was used to collect images of asphalt pavement after paving and compaction according to the set parameters. The images collected were preprocessed in steps such as binary grayscale, filtering, histogram, and small particle filtering, which established the method for calculating the construction depth H_P of the digital images of pavement. Moreover, a method was proposed to evaluate the uniformity of asphalt pavement using the construction depth coefficient of variation. The coefficients of variation were computed based on 100 images of the dependent project and compared with the actual images. The results indicated that the construction depth coefficient of variation of the digital images obtained by the developed calculation procedure was in agreement with the actual situation and combined the correlation degree of the calculation results. Small areas of 4^2 are recommended as the division of the asphalt pavement compaction uniformity evaluation method based on construction depth variation, and the use of $C_{v4} \geq 8.0$ as the evaluation standard for the segregation of asphalt pavement is recommended. The method proposed is a new and rapid test to evaluate and detect the asphalt pavement uniformity.

1. Introduction

The segregation of asphalt mixtures is a common issue to asphalt concrete pavement surfaces. This segregation is accelerated by the dynamic load of vehicles, resulting in the development of potholes and pileups, which affect both the aesthetics and performance of the pavement in serious cases [1, 2]. Thus, the segregation of asphalt mixtures after paving is one of the root causes of local damage of asphalt concrete pavement [3].

Many studies have been conducted by domestic and international scholars to determine the segregation of asphalt mixture. The uniformity of asphalt mixtures mainly refers to the uniformity of distribution of coarse and fine aggregates [4]. Brock [5] stated that pavement segregation can lead to changes in mixture gradation and asphalt content, resulting in poor pavement structural performance. Kennedy et al. [6] analysed the phenomenon and mechanism of asphalt mixture segregation and proposed that it is related to the nonuniform dispersion of coarse and fine aggregates. Nondestructive technologies have been developed for the identification and evaluation of asphalt mixture homogeneity, such as thermal infrared imager, ground penetrating radar, and laser surface profiler [7–9]. Gilbert [10] used a thermal infrared imager to test the temperature distribution of the asphalt mixture during the construction process to reflect the degree of mixture segregation. The author found that the temperature of the asphalt mixture did not necessarily lead to aggregate segregation. Schmitt et al. [11] and Liu [12] used pavement ground-penetrating radar, which can determine the distribution of density of asphalt concrete pavement.

As a new interdisciplinary technology, the birth of digital image processing can be dated back to the 1960s and has become increasingly mature along with the development of computer technology and digital signal processing technology. In recent years, digital image processing technology has developed rapidly in the field of road engineering and has been applied to the quantitative evaluation of asphalt mixture uniformity research [13, 14]. Azari [15] verified the characteristics of aggregate distribution in computed tomography scan images of asphalt mixture specimens using the normal distribution method in statistics. If the distribution characteristics satisfied the standard normal distribution, the distribution was found to be uniform. Bruno et al. [16] analysed the gradation of aggregates by digital image acquisition of core samples after drilling and core samples of on-site asphalt pavement and extracted the aggregate particles in the core samples using a digital image method.

Considering the abovementioned studies, the application of digital image technology in asphalt mixtures has been mainly used to evaluate and analyse aggregate particle uniformity and asphalt mixture paving uniformity, whereas few studies have focused on the uniformity of asphalt mixture after paving and compaction and its correlation analysis with traditional methods. Therefore, in this study, for the asphalt mixture compaction stage, digital image processing technology was used to construct the relationship between the construction depth in the traditional sand paving method and the construction depth using digital image processing. The evaluation method of asphalt pavement compaction uniformity based on the construction depth variation was proposed to evaluate the compaction uniformity of asphalt pavement with the variation coefficient as the evaluation index.

2. Image Acquisition and Processing Technology

2.1. Image Acquisition. Acquisition of images is the first step in evaluating the uniformity of aggregate distribution in asphalt mixtures. The sketch of asphalt mixture image acquisition and calculation is shown in Figure 1. In this study, the image acquisition was tested on a sunny day, the metal oxide semiconductor COMS industrial camera in Figure 2 height from the asphalt mixture paving surface was 60 cm, and the front is vertical downward. The area of paving asphalt mixture captured by each image was measured to be 72 cm × 72 cm. The image pixel resolution was 2448 × 2448 according to the performance of the COMS industrial camera used for image acquisition at the construction site, shooting height, etc.

2.2. Image Preprocessing. To calculate the statistical analysis of the collected asphalt mixture images, the photos need to be processed. We collected photos of the middle pavement surface layer AC-20 asphalt mixture (The pavement asphalt layer has three layers, the lower layer is ATB-30, the middle layer is AC-20, and the upper layer is AC-16.) at Shiyan highway after paving and compaction. A total of 586 photos (shooting without overlap) were preprocessed. Figure 3 shows an example of the preprocessing, taking photo SY-001 as an example, where SY denotes the name of Shiyan highway, and 001 denotes the photo number.

The acquired raw images were preprocessed by MATLAB software, and the processing steps were as follows: (1) greying the colour images using the rgb2gray function; (2) Use function medfilt2 for spatial filtering and denoising removal to improve the image quality; (3) histogram equalization to enhance the image contrast and improve the image clarity; (4) morphological processing and watershed segmentation of the histogram equalized images to identify and segment the adherent particles. After this process, the final binary image was obtained (Figure 3(b)).

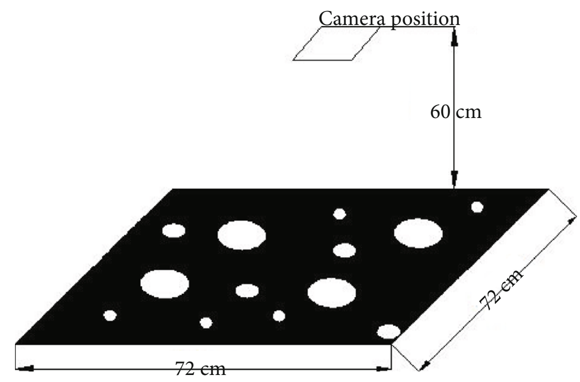

Figure 1: Sketch of pavement image acquisition and calculation.

Figure 2: COMS industrial camera.

3. Calculation Method of Construction Depth of Asphalt Pavement

3.1. Computational Model. As the surface of asphalt pavement is rough and uneven, light irradiation on the pavement will be diffusely reflected, and the light intensity of diffuse reflection will vary with the roughness of the middle pavement surface. Therefore, when the camera is used to capture the image of asphalt mixture, different light intensities are displayed differently in the image.

In this study, asphalt mixture compaction was the research object and the shooting occurred in natural light on a clear day. Studies reported that there is a linear relationship between the grayscale value and the construction depth (i.e., the greater the pavement construction depth, the smaller the grayscale value of the image) [17]. Therefore, digital image processing technology was used to calculate the depth of asphalt pavement construction. The average construction depth of the pavement image was calculated

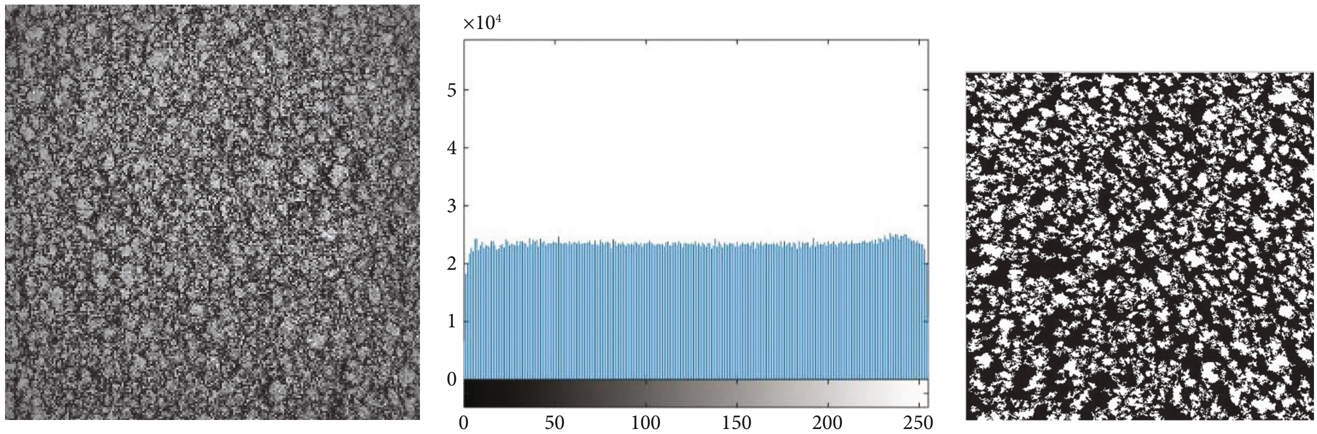

(a) SY-001 original image (b) Histogram of SY-001 after equalization (c) SY-001 binarized postprocessed image

Figure 3: Image processing.

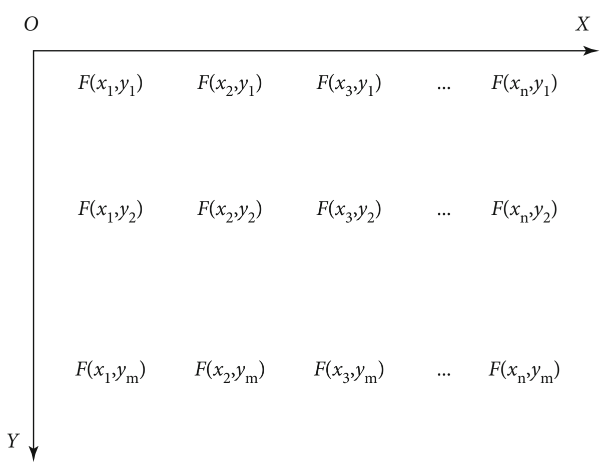

Figure 4: 2D numerical matrix of the grayscale image.

by reflecting the convexity of the asphalt pavement surface by the brightness and darkness of the image pixels, and the difference in height between the raised and concave pavement was reflected by the grayscale difference to construct a three-dimensional (3D) surface [18].

The pavement images acquired through the camera were red-green-blue images, which could be represented after preprocessing by MATLAB toolbox functions as an $m \times n$ of a two-dimensional (2D) matrix. If $Z_{ij} = (X_i, Y_j)$, then a 3D surface could be constructed (i.e., the surface texture construction map of the asphalt pavement). Figures 4 and 5 show the 2D matrix of the asphalt pavement image and the 3D surface of the asphalt pavement surface image, respectively.

Based on the data from the 2D matrix, the pavement construction depth was calculated as

$$Z = F(x, y), \tag{1}$$

$$V = \iint_D [F_{\max} - F(x, y)]\, \mathrm{dxdy}, \tag{2}$$

where Z is the pixel value; (x, y) are the horizontal and vertical coordinates corresponding to the pixel, respectively; V is the volume of space enclosed by the pixel value of the surface construction; $F_{\max}$ denotes the largest grey value in the grey matrix; $F(x, y)$ is the grey value of the pixel point whose coordinates are (x, y); the integration region D is equivalent to the sand spreading range in the sand spreading method; V_p is the volume enclosed by the spatial surface and plane $F_{\max}$ of the pavement surface construction, which is equivalent to the sand spreading volume in the sand spreading method.

Digital image processing technology was used to calculate the digital construction depth H_p of the pavement to characterize the roughness. The higher the H_p value, the rougher the pavement. The formula for calculating the digital construction depth H_p of the pavement is

$$H_p = \frac{V}{D}, \tag{3}$$

where D is the integral region, calculated as the product of the number of rows and columns of the matrix.

The pavement surface construction depth H_p needs to be corrected by the scale correction factor μ to obtain the final digital construction depth H' of the asphalt pavement surface. The calculation formulas are

$$\mathrm{H}^{'} = \frac{H_P}{\mu} = \frac{H_P}{(Z_{\max} - Z_{\min})/\alpha}, \tag{4}$$

$$\mu = \frac{Z_{\max} - Z_{\min}}{\alpha}, \tag{5}$$

where $Z_{\max}$ and $Z_{\min}$ are the maximum and minimum values of all elements in the matrix Z, respectively; α is the empirical coefficient and takes the value of 1.36.

3.2. Calculation Procedure for the Coefficient of Variation of the Construction Depth

3.2.1. Calculation Method. The asphalt pavement images can be divided into equal parts by 2^2, 3^2, 4^2, 5^2, and 10^2 as shown in Figure 6, and the mean depth of construction, variance

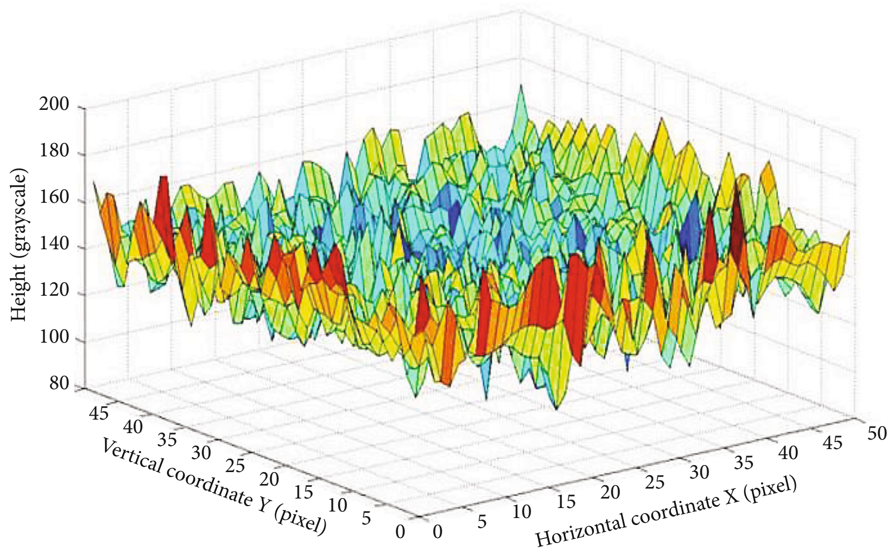

Figure 5: 3D surface of asphalt pavement surface image.

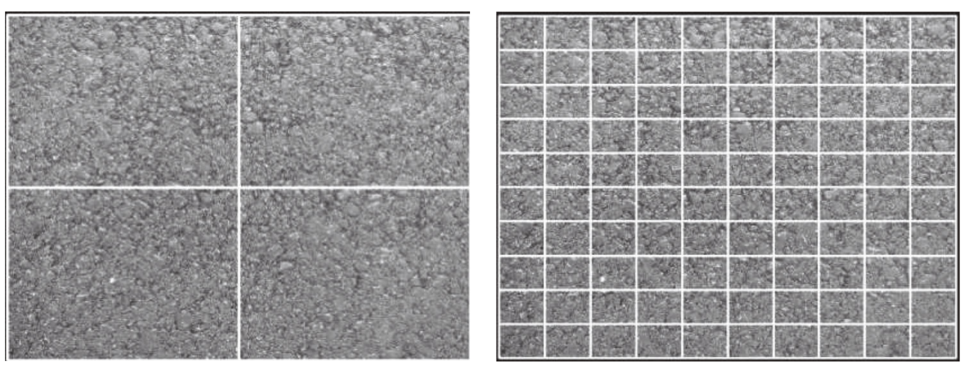

(a) 2^2 division method

(b) 10^2 division method

Figure 6: Area division method for pavement images.

between regions (S) and coefficient of variation (C_v), is calculated for each equal part of the area. The calculation formulas are

$$\bar{H}_p = \frac{\sum_{i=1}^{n} H_{\mathrm{Pi}}}{n}, \tag{6}$$

$$S = \sqrt{\frac{\left(H_{\mathrm{Pi}} - \bar{H}_P\right)^2}{n-1}}, \tag{7}$$

$$C_v = \frac{S}{H_P \times 100}, \tag{8}$$

where H_{Pi} is the average digital construction depth of each aliquot (mm); $\bar{H}_P$ is the average digital construction depth of the image (mm); n is the number of small regions divided, $n = 4, 9, 16, 25, 100$.

3.2.2. Procedure for Calculating Coefficients of Variation for Digital Image Construction Depth. In this study, MATLAB software was used to write a fast procedure for calculating the coefficient of variation of the construction depth from asphalt pavement.

MATLAB software was run, and the pavement digital construction depth discrepancy coefficient of variation calculation program, whose main interface is shown in Figure 7, was loaded. The main functions of this calculation program include create task, load image, automate, draw pavement texture construction map, and calculate and export, which are controlled by five buttons on the main interface.

4. Correlation Analysis of the Coefficient of Variation (C_v) and Aggregate Segregation

4.1. Correlation Analysis of Coefficient of Variation of Construction Depth from Digital Images. The acquired images of the medium surface AC-20 asphalt mixture compacted pavement were imported into the MATLAB calculation program. The images were segmented according to five different aliquot methods of 2^2, 3^2, 4^2, 5^2 and 10^2, and the coefficient of variation C_v of the pavement digital image

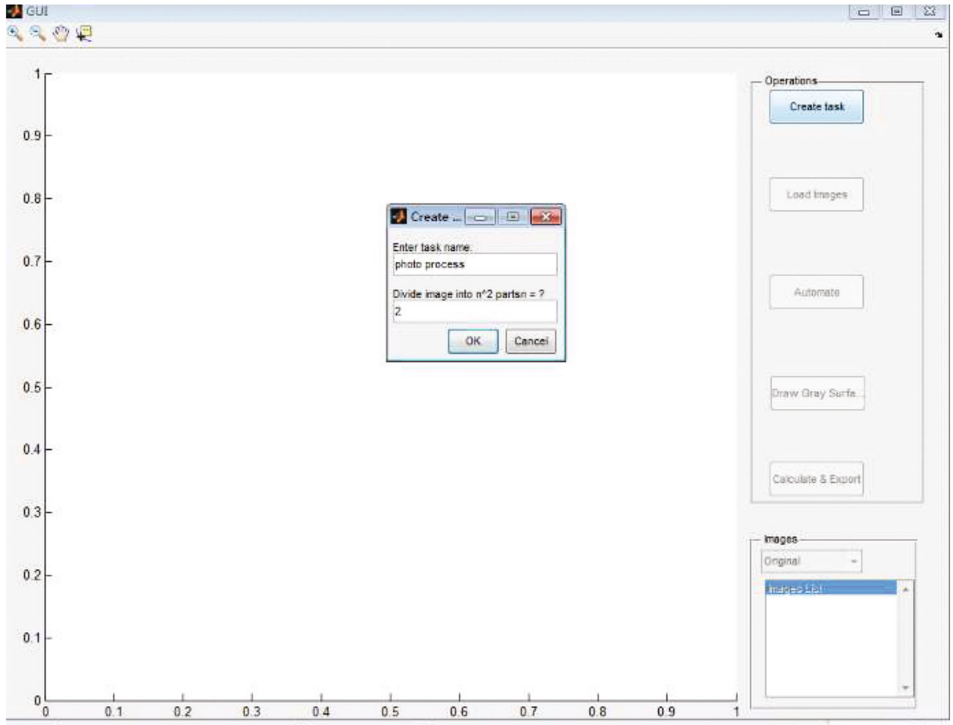

Figure 7: Main interface of the calculation program.

construction were calculated separately. The calculation results are shown in Table 1.

The calculated results of the C_v values were compared to the corresponding asphalt pavement images by visual observation and were overall consistent with the expected assumption that the higher the C_v value for the digital image construction of the asphalt pavement, the higher the likelihood of aggregate segregation. This tendency can be observed in Figures 8(a) and 8(b) for uniformity of mix compaction and inhomogeneity, respectively. The C_v results of the computation of the construction depth coefficient of variation in Table 1 were as follows: Figure 8(a), $C_{v2} = 2.12$, $C_{v3} = 2.76$, $C_{v4} = 3.57$, $C_{v5} = 3.37$, $C_{v10} = 3.84$; Figure 8(b), $C_{v2} = 12.75$, $C_{v3} = 12.94$, $C_{v4} = 1\,3.35$, $C_{v5} = 13.16$, $C_{v10} = 14.08$. Thus, the values were corroborated with the visually observed uniformity of the asphalt pavement aggregate distribution.

Table 1: Depth of departure coefficient of variation for digital image construction of AC-20 asphalt mixture pavement.

Number	C_{v2}	C_{v3}	C_{v4}	C_{v5}	C_{v10}
1	4.68	5.04	5.18	5.39	5.60
2	3.17	4.44	5.66	5.65	6.48
3	4.38	5.92	5.65	5.76	6.02
4	4.29	4.81	4.69	5.35	5.43
5	7.86	7.38	7.12	7.09	7.29
6	3.15	3.87	3.55	4.24	4.88
7	2.15	2.77	2.41	2.59	2.80
8	3.58	3.29	4.49	4.60	5.47
9	5.49	6.02	6.04	6.46	6.98
10	5.35	5.78	5.09	5.51	5.51
11	2.12	2.76	3.57	3.37	3.84
……	……	……	……	……	……
93	3.16	3.29	3.36	2.97	3.80
94	6.46	6.71	6.65	6.69	7.02
95	10.52	9.95	9.98	10.32	10.46
96	5.88	6.35	6.31	6.42	6.42
97	3.46	3.77	3.37	3.81	4.10
98	5.33	5.42	5.33	5.21	5.18
99	6.31	5.80	5.80	5.92	6.20
100	7.35	7.16	7.12	6.79	7.30

4.2. Correlation Analysis of Depth Coefficient of Variation for Digital Image Construction with Different Equal Area Division Methods. The digital image construction depth coefficient of variation C_v can be calculated according to five image segmentation methods of 2^2, 3^2, 4^2, 5^2, and 10^2. From Table 1, the C_v values of the five segmentation methods of each image were different, but from the overall analysis of the 100 acquired asphalt pavement images, they showed a certain correlation. Therefore, a correlation analysis between two C_v values was conducted, and a more stable and representative partitioning method was selected as the standard for calculating the coefficient of variation for asphalt pavements based on the results of the correlation analysis.

Taking the image divided by 2^2 and 3^2 as an example, the distribution of the digital image construction depth coefficients of variation C_{v2} and C_{v3} is shown in Figure 9. As observed, the same image divided by 2^2 and 3^2 division

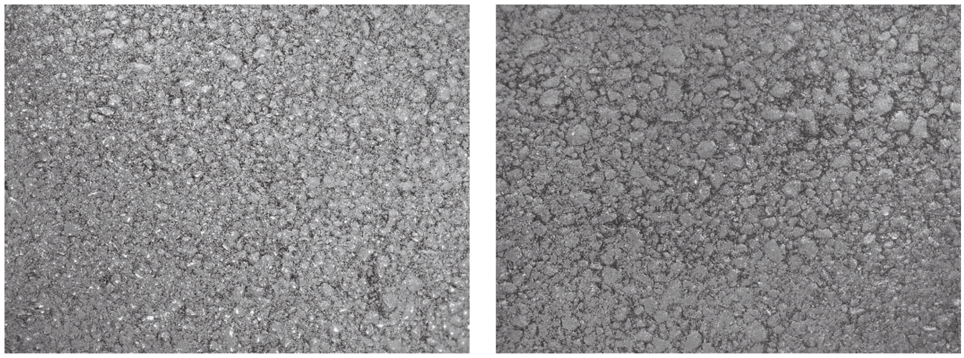

(a) TXYS-11 undissociated image (b) TXYS-95 dissociated image

Figure 8: Raw photos from image acquisition.

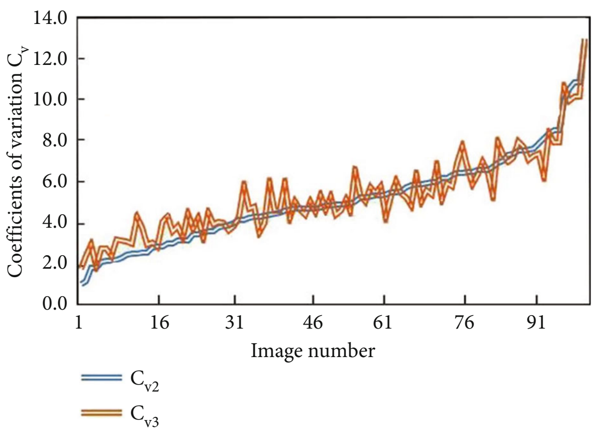

Figure 9: Distribution of coefficients of variation C_{v2} vs. C_{v3}.

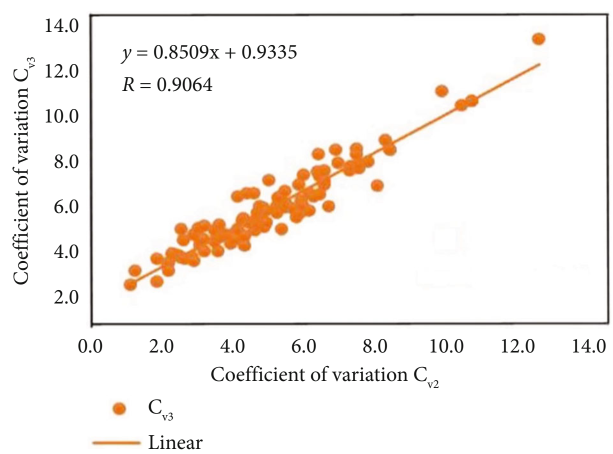

Figure 10: Correlation between coefficients of variation C_{v2} and C_{v3}.

methods correspond to different construction depth coefficients of variation C_{v2} and C_{v3}, respectively. However, from the overall analysis of 100 asphalt pavement images, the tendency of the construction depth coefficients of variation C_{v2} and C_{v3} is consistent. A linear regression with C_{v2} as the independent variable X and C_{v3} as the variable Y is shown in Figure 10. The linear regression equation is $Y = 0.8509X + 0.9335$, and the squared correlation coefficient is $R^2 = 0.91$. Thus, there is a good linear correlation between C_{v2} and C_{v3}.

Using the same method, the linear regression equations and square of the correlation coefficients were obtained by constructing a correlation analysis of the coefficients of variation C_{v2}, C_{v3}, C_{v4}, C_{v5}, and C_{v10} for the digital images, as shown in Table 2.

From Table 2, the square of the correlation coefficient R^2 between C_{v2} and C_{v3}, C_{v4}, C_{v5}, C_{v10} ranged between 0.83 and 0.91, whereas the squares of the correlation coefficients R^2 between C_{v3}, C_{v4}, C_{v5}, C_{v10} and the other four division methods ranged between 0.91–0.96, 0.89–0.98, 0.88–0.98, and 0.83–0.98, respectively. Thus, the correlations between the division methods of 2^2 and 10^2 and the other four division methods were relatively weak, whereas there was a strong correlation between the coefficients of variation from the construction depth of digital image calculated by aliquoting images by 3^2, 4^2, and 5^2 division methods. Considering

Table 2: Correlation relationships of digital image construction depth coefficients of variation C_{v2}, C_{v3}, C_{v4}, C_{v5}, and C_{v10}.

Independent variable	Variable	Linear regression equation (Math)	Square of correlation coefficient R^2
C_{v2}	C_{v3}	$C_{v3} = 0.8509C_{v2} + 0.9335$	0.9064
	C_{v4}	$C_{v4} = 0.8336C_{v2} + 1.1385$	0.8851
	C_{v5}	$C_{v5} = 0.8086C_{v2} + 1.3984$	0.8750
	C_{v10}	$C_{v10} = 0.782C_{v2} + 1.8718$	0.8297
C_{v3}	C_{v4}	$C_{v3} = 0.9735C_{v4} + 0.2566$	0.9642
	C_{v5}	$C_{v3} = 0.9467C_{v5} + 0.5305$	0.9580
	C_{v10}	$C_{v3} = 0.212C_{v10} + 1.0028$	0.9195
C_{v4}	C_{v5}	$C_{v4} = 0.9663C_{v5} + 0.3141$	0.9810
	C_{v10}	$C_{v4} = 0.9479C_{v10} + 0.7509$	0.9570
C_{v5}	C_{v10}	$C_{v5} = 0.981C_{v10} + 0.4427$	0.9755

that the more regions are divided, the slower their operation speed, and combined with the correlation degree of the calculation results, we determined that the best evaluation method of asphalt pavement compaction uniformity based

Table 3: Images of AC-20 asphalt mixture pavement with coefficient of variation $C_{v4} \geq 8.0$.

Project name	C_{v2}	C_{v3}	C_{v4}	C_{v5}	C_{v10}
	TXYS-70			TXYS-22	
	TXYS-53	TXYS-22	TXYS-53	TXYS-53	TXYS-68
	TXYS-21	TXYS-53	TXYS-95	TXYS-21	TXYS-53
	TXYS-51	TXYS-95	TXYS-15	TXYS-51	TXYS-95
Image number	TXYS-20	TXYS-15	TXYS-30	TXYS-15	TXYS-15
	TXYS-95	TXYS-30	TXYS-20	TXYS-30	TXYS-30
	TXYS-15	TXYS-20	TXYS-39	TXYS-95	TXYS-20
	TXYS-30	TXYS-39		TXYS-20	TXYS-39
	TXYS-39			TXYS-39	
Number of images	9	7	6	9	7

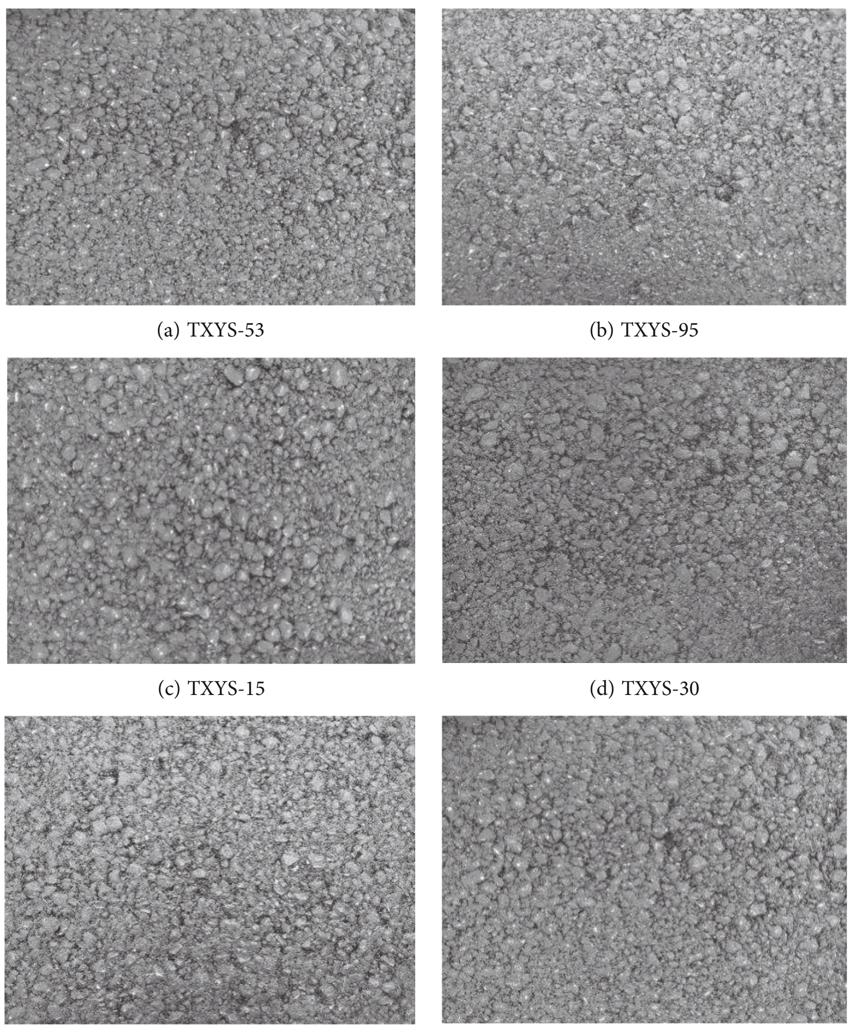

(a) TXYS-53
(b) TXYS-95
(c) TXYS-15
(d) TXYS-30
(e) TXYS-20
(f) TXYS-39

Figure 11: Acquisition images of aggregate segregation in asphalt pavements.

on the construction depth variation consists of dividing the image into 4^2 small areas.

4.3. Evaluation Criteria Based on the Coefficient of Variation of the Construction Depth. According to the results of the coefficient of variation C_{v4} of the construction depth based on asphalt pavement images calculated using MATLAB, combined with the visual observation of the asphalt pavement aggregate distribution uniformity, it was found that when C_{v4} took a value close, equal, or greater than 8, there was a relatively evident segregation of the asphalt pavement aggregate distribution based on visual observation. As a result, the preliminary evaluation criterion of asphalt pavement segregation was set to $C_{v4} = 8.0$.

For $C_{v4} = 8.0$, the corresponding C_{v2}, C_{v3}, C_{v5}, and C_{v10} values were calculated according to the correlation relationship equation in Table 2 as 7.875, 7.907, 8.071, and 8.334, respectively. From the calculated 100 asphalt pavement images, the images with values of C_{v2}, C_{v3}, C_{v5}, and C_{v10} greater than or equal to 8 were selected. After screening, those with a coefficient of variation of $C_{v4} \geq 8.0$ are presented in Table 3.

Using $C_{v4} = 8.0$ as the boundary value of aggregate segregation for the following layer of AC-20 asphalt mixture pavement, six asphalt pavement images were screened, and the asphalt pavement corresponding to these six images was considered to exhibit aggregate segregation, as shown in Figure 11. By observation, these asphalt pavements exhibited a more evident coarse and fine aggregate separation, indicating that the use of $C_{v4} = 8.0$ for aggregate inhomogeneity determination was in accordance with the actual situation.

5. Conclusions

In this study, the compaction uniformity of asphalt pavement was evaluated based on the construction depth segregation for the compacted pavement of AC-20 asphalt mixture using digital image processing technology and MATLAB software programming. The main findings include

(1) A calculation method for calculating the construction depth H_p of digital images of pavements was established by characterizing the height difference between raised and depressed pavements in terms of the image grayscale difference, and a method for evaluating the uniformity of asphalt pavements using the construction depth coefficient of variation was proposed

(2) A program was written in MATLAB to quickly calculate the digital construction depth coefficients of variation for pavements, and the coefficient of variation was also calculated for 100 images of the dependent project and compared with the actual images; it was found that the coefficients of variation calculated by the developed program were in accordance with the actual situation

(3) By analysing the correlation between different division regions two by two, it was found that the correlation between 2^2 and 10^2 division methods was weak, whereas the division methods of 3^2, 4^2, and 5^2 exhibited strong correlations. Combined with the operation speed, a small area of 4^2 is recommended as the division method of asphalt pavement compaction uniformity evaluation based on the construction depth variation

(4) By visually comparing and analysing the observed and calculated values, it is recommended to use $C_{v4} \geq 8.0$ as the evaluation criterion for asphalt pavement segregation

Data Availability

The data used and/or analysed during the current study are available from the corresponding author on reasonable request.

Conflicts of Interest

The author declares that there is no conflict of interest to report regarding the present study.

Acknowledgments

This work was supported by the Chongqing Natural Science Foundation Project (Grant no. cstc2020jcyj-msxmX0320) and the Science and Technology Research Program of Chongqing Municipal Education Commission (Grant No. KJQN202104001).

References

[1] W. Qin, *Study on Segregation of Pavement Materials Based on Granular Characteristics*, Chang'an University, 2011.

[2] H. Zhu, *Research on Application of New Method for Quick Evaluation of Segregation of Asphalt Mixture*, vol. 32, no. 1, 2016Highway Traffic Technology, 2016.

[3] S. L. Li, N. X. Liang, and S. Zeng, "Influence of acquisition methods on segregation evaluation of digital image of asphalt mixture," *Journal of Chongqing Jiaotong University (Natural Science)*, vol. 40, no. 3, pp. 103–107, 2021.

[4] Y. F. Luo, J. Q. Zhang, and C. Zhang, "Sensitivity analysis of factors influencing shear stress in asphalt pavements under high temperature conditions," *Journal of Wuhan University (Engineering Edition)*, vol. 51, no. 10, pp. 895–900, 2018.

[5] J. D. Brock, *Segregation of Asphaltic Mixtures (with Discussion)*, Association of Asphalt Paving Technologists Proc, 1986.

[6] T. W. Kennedy, R. B. Mcgennis, and R. J. Holmgreen, *Asphalt Mixture Segregation: Diagnostics and Remedies (with Discussion)*, Association of Asphalt Paving Technologists Proc, 1987.

[7] M. Lesturgie and H. Griffiths, "Guest editorial special issue: "catching the invisible"," *IET Radar, Sonar & Navigation*, vol. 10, no. 1, pp. 1-2, 2016.

[8] B. Hui, M. Guo, and X. F. Liu, "Quality assessment of milling pavement surface using 3D line laser technology," *Journal of South China University of Technology (Natural Science Edition)*, vol. 2018, no. 11, pp. 1–9, 2018.

[9] L. Q. Hu, Y. B. Tuan, and T. L. Wang, "Analysis of temperature uniformity of asphalt mixture paving based on thermal imaging," *Journal of Jiangsu University (Natural Science Edition)*, vol. 37, no. 6, pp. 735–739, 2016.

[10] K. Gilbert, *Thermal Segregation*, Binders, 2005.

[11] R. L. Schmitt, A. Faheem, and I. L. Al-qadi, "Selection of non-destructive testing technologies for asphalt pavement construction," in *Airfield & Highway Pavement Conference*, Los Angeles, California, United States, 2013.

[12] T. Liu, *Research on the Evaluation of Dielectric Properties and Construction Quality of Asphalt Pavement Based on Non-*

Destructive Testing Methods, South China University of Technology, 2016.

[13] W. L. Wu, Z. Li, and X. N. Zhang, "Evaluation of asphalt mixture uniformity by digital image processing technique," *Journal of Jilin University (Engineering Edition)*, vol. 39, no. 4, pp. 921–925, 2009.

[14] J. Ma, X. M. Zhao, and S. H. He, "A review of road surface inspection techniques," *Journal of Transportation Engineering*, vol. 17, no. 5, pp. 121–137, 2017.

[15] H. Azari, *Effect of Aggregate Inhomogeneity on Mechanical Properties of Asphalt Mixtures*, R. Mccue, Ed., vol. 66-12 of Dissertation Abstracts International, 2005.

[16] L. Bruno, G. Parla, and C. Celauro, "Image analysis for detecting aggregate gradation in asphalt mixture from planar images," *Construction & Building Materials*, vol. 28, no. 1, pp. 21–30, 2012.

[17] Y. M. Liu, S. Han, and O. M. Xu, "Acquisition system for three-dimensional surface texture of asphalt pavement based on digital image processing," *Journal of Southwest Jiaotong University*, vol. 49, no. 2, pp. 351–357, 2014.

[18] D. Cheng, *Study on Image-Based Texture Analysis Method and Prediction of Skid-Resistance & Tire/Pavement Noise Reduction of HMA*, Chang'an University, 2015.